XI. SPONTANEOUS RADIOFREQUENCY EMISSION FROM HOT-ELECTRON PLASMAS*

Academic and Research Staff

Prof. A. Bers

Graduate Students

C. E. Speck

A. SPATIAL DISTRIBUTION OF THE VISIBLE LIGHT GENERATED IN A PULSED ELECTRON-CYCLOTRON RESONANCE DISCHARGE

We are continuing the experimental study of a pulsed electron-cyclotron resonance discharge that exhibits an intense microinstability in the afterglow. In this report, we present measurements of the spatial distribution of the light intensity generated by electron excitation of the neutral background gas. From these measurements a new estimate of the volume of the plasma is presented.

1. Radial Dependence of the Light

The radial dependence of the light intensity generated by a rotationally symmetric plasma may be determined from the measurement of the light generated along chords of the plasma column. Transformation between the intensity as a function of the distance of the chord from the center of the plasma and intensity as a function of radius is achieved by the employment of the Abel Transform[1]:

$$I(r) - I(r_{max}) = -\frac{1}{\pi}\int_{r}^{r_{max}} \frac{I'(z)\,dz}{(z^2-r^2)^{1/2}}.$$

Here I(r) is the radial intensity variation, I(z) is the light intensity from a chord a distance z from the center of the column, and I'(z) = dI(z)/dz. The experimental plasma is expected to be rotationally symmetric in the afterglow, since any spatial structure caused by the RF heating should be removed by the azimuthal grad-B drifts.

Since the plasma is generated within an opaque microwave cavity, a direct measurement of I(z) along chords perpendicular to a particular radius could not be made. Indirectly, however, this information was obtained from the system illustrated in Fig. XI-1. A stainless-steel mirror located within the vacuum chamber reflects light from the cord defined by the angle α into a fixed light collimator. The angle α is continuously

*This work was supported by the United States Atomic Energy Commission under Contract AT(30-1)-3581.

adjustable from outside the cavity by means of a gear assembly driven by a shaft passing through a Veeco vacuum seal. A measurement of the intensity as a function of the angle α can then be transformed to that as a function of z by noting that $z = d \sin \alpha$, where d is the known distance of the mirror from the center of the plasma.

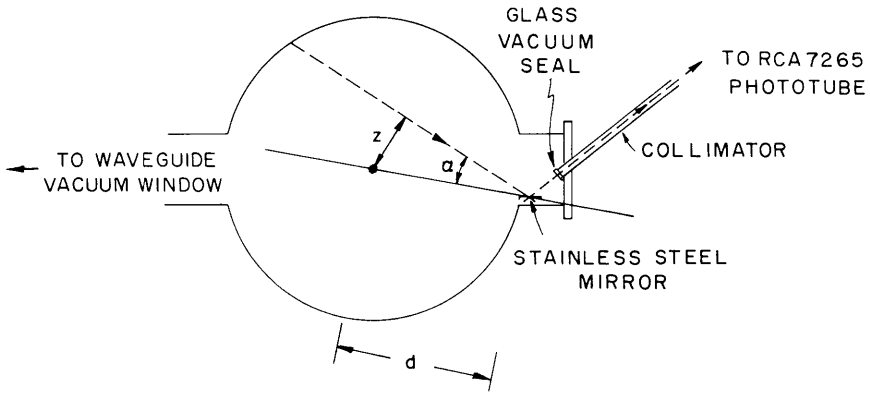

Fig. XI-1. Experimental apparatus for measurement of the radial light intensity.

At the low background gas pressures used in these experiments ($\sim 2 \times 10^{-5}$ Torr H_2) very little visible light is generated by the plasma. Collimation further reduces the available light. In order to measure the light, a rather sensitive photomultiplier tube was necessary (RCA 7265). Furthermore, the determination of meaningful relative intensity measurements required that this noisy light signal be averaged over many plasmas in order to eliminate plasma-to-plasma variations in the light output. This was accomplished with a PAR Model CW-1 boxcar integrator. In operation, the input to the integrator was gated on for a 10-μsec interval at a fixed time following the end of the microwave heating pulse. The mirror was continuously rotated by means of a geared-down 1 rpm motor, with the result that the angle α was scanned at the rate of 24°/minute. A precision potentiometer was connected to the shaft driving the mirror to provide a resistance proportional to the angular deflection of the mirror. The use of this resistance in a voltage divider circuit produced a voltage proportional to the angle α. This signal was used to drive the x-axis of an x-y recorder, while the averaged light signal from the output of the integrator drove the y-axis. Plots of the intensity as a function of the angle α were obtained in this manner at several values of delay time following the end of the microwave heating pulse. A typical plot of the experimental data is shown in Fig. XI-2.

In transforming the data to intensity as a function of radius the approach of Freeman and Katz was employed.[2] A least-squares approximation of an m^{th}-degree polynomial of the form

$$I(z) = \sum_{k=0}^{m} F_k \left(r_{max}^2 - z^2\right)^k$$

was fitted to the experimental data. Here r_{max} is taken to be the radius at the cavity wall and the F_k are coefficients determined by the fitting procedure. The assumed

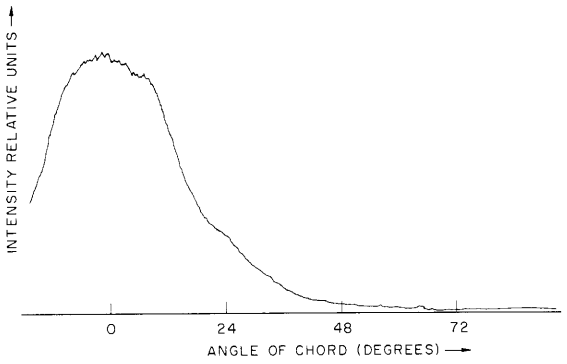

Fig. XI-2.

Measured light intensity vs angular location of the observed chord 10 μsec after the end of the microwave heating pulse.

form of I(z), when substituted in the Abel transform, can be integrated analytically to yield

$$I(r) - I(r_{max}) = \frac{1}{\pi} \sum_{k=1}^{m} kF_k \frac{\Gamma(1/2)\,\Gamma(k)}{\Gamma(k+1/2)} \left(r_{max}^2 - r^2\right)^{k-1/2},$$

where Γ is the well-known gamma function.

Figures XI-3 and XI-4 present the results of the transformation when applied to the experimental data taken before and after the instability, respectively. Under the conditions of operation stated in Fig. XI-3, the most probable time of occurrence of the instability was 200 μsec following the end of the heating pulse. First, note that the light is not peaked at the center of the plasma. Furthermore, near r = 10 cm the decrease of intensity with radius becomes less rapid. At a heating frequency of 2852 MHz and a current of 71 A in the magnets, the magnetic field at r = 9.8 cm in the midplane is one half of the field required for cyclotron resonance with the heating frequency. The less rapid decrease in the light intensity near r = 10 cm may be evidence of heating at the second harmonic of the cyclotron frequency. Similar, but much more pronounced, effects have been observed by others.[3] At a radius of 15.6 cm, the magnetic field has fallen to such a value that the local electron-cyclotron frequency is one third of the heating frequency. The light intensity near this radius exhibits another flat region that may be indicative of third-harmonic heating. The occurrence of the main peak of the intensity at r $\cong$ 3 cm is still not understood. The magnetic-field contour corresponding

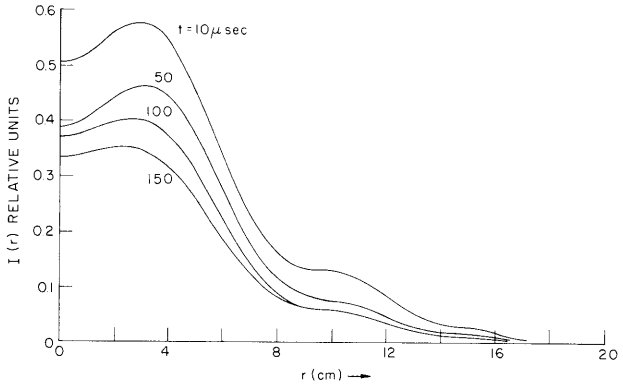

Fig. XI-3. Radial distribution of the visible light intensity at times before the instability. Parameter indicates the time after the end of the microwave heating power. Discharge conditions: 1.8×10^{-5} Torr H_2, magnet current = 71 A, and incident heating power is 32 kW peak at 2852 MHz.

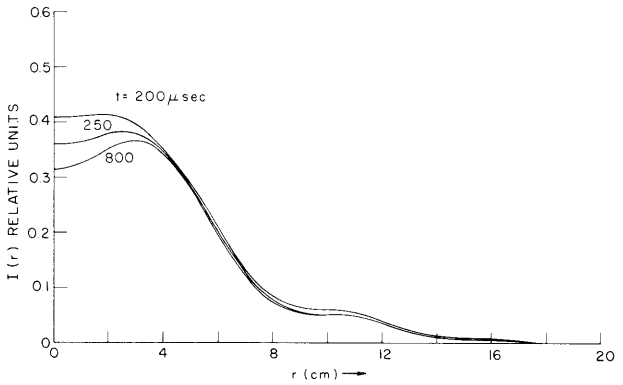

Fig. XI-4. Radial distribution of the visible light intensity at times after the instability. Conditions identical with those of Fig. XI-3.

to fundamental cyclotron resonance at the heating frequency does not pass through the midplane of the cavity. Possibly, it follows from the field structure of the cavity mode near 2852 MHz.

The time dependence of the radial light intensity shows that just before the instability the entire distribution is decaying. The greatest decay rates occur, however, at radii near the peak of the distribution and tend to flatten it. The occurrence of the instability causes an increase in the light output at all radii, although the greatest charges occur for radii less than 6 cm. The increase in light is probably due to cyclotron resonance heating of the cold background electrons to a few tens of Volts by the instability radiation. Following the instability, the intensity decays much slower than before with most of the variation occurring at radii less than 3 cm.

2. Axial Dependence of the Light

The axial dependence of the light generated by the plasma was determined with the apparatus illustrated in Fig. XI-5. The front port of the cavity was closed with a plexiglas vacuum window. Inside the cavity, just behind the window, was a copper screen. The mesh of the screen was fine enough to effectively be a microwave short, but still allowed for a high transmission of visible light. A precision turntable was employed to accurately rotate the phototube-collimator assembly so as to view different locations along the axis of the cavity. A deflection of approximately 16° was required to move the viewed location from one end of the cavity to the other. Knowing the distance of the phototube from the center of the cavity, L, and the angle of deflection, ϕ, we can find the axial location from

$$z = L \tan \phi.$$

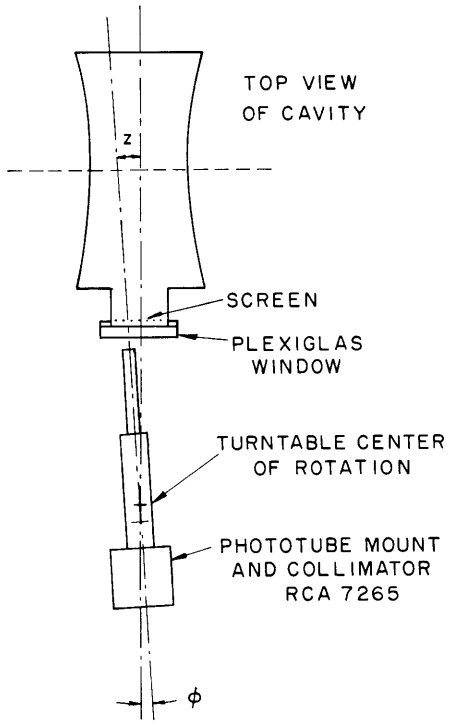

Fig. XI-5. Experimental apparatus for measurement of the axial light intensity.

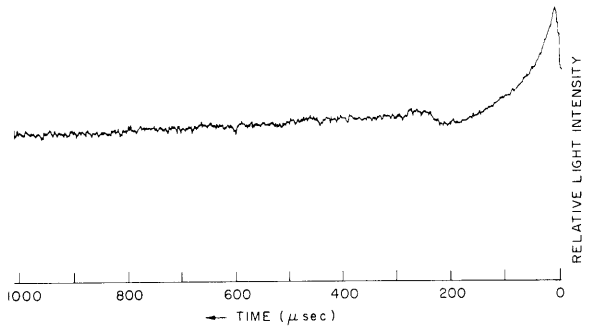

Fig. XI-6. Light intensity vs time following the end of the microwave heating power at a fixed axial position.

As in the radial intensity measurements, a PAR boxcar integrator was used to average the phototube output over many plasmas. In these measurements the turntable was fixed at a particular axial position, and the time, with respect to the end of the heating pulse, at which the integrator was gated on was slowly scanned. Figure XI-6 presents a typical time dependence of the light near the center of the discharge. Note the similarity between the average behavior of the light as presented in Fig. XI-6 and the previously reported behavior of the light signal during a single plasma.[4] In each case, the light intensity falls rapidly following the end of the heating

pulse up to the time of the instability (soon after 200 μsec). Following the instability, the light rises to a slightly higher value and then begins a relatively slow decay. As previously reported,[4] if the plasma is not reheated at t = 1000 μsec, the light signal continues to decay at this slow rate for several tens of milliseconds.

Data similar to that in Fig. XI-6 were taken at several axial positions. These data have been combined in Figs. XI-7 and XI-8. Note that before the instability (Fig. XI-7),

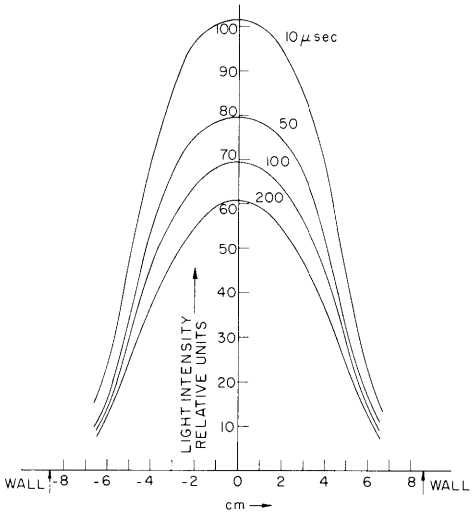

Fig. XI-7. Axial distribution of the visible light intensity before the instability. Discharge conditions as stated in Fig. XI-3.

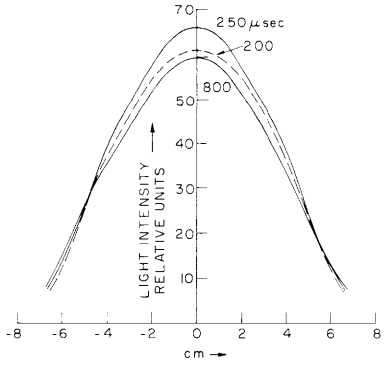

Fig. XI-8. Axial distribution of the visible light intensity after the instability compared with that just before the instability (t=200 μsec).

the distribution decays uniformly at all axial positions. In Fig. XI-8, the distribution at two times following the instability is compared with that just before. Note that 50 μsec after the instability the light has increased over that before at all axial positions. The greatest change occurs, however, at the center of the plasma. At even later times, the intensity near the center has fallen below the intensity before the instability. But beyond approximately 5 cm from the center, the intensity is still greater than that before.

The electrons responsible for the increase in light just after the instability appear to be initially concentrated near the center of the plasma. As time goes on, however, they appear to begin to move farther out into the mirror regions. This picture is consistent with electron-cyclotron resonance heating of the cold-electron background by the instability radiation. Such a process tends to selectively add energy to the motion of the electrons transverse to the static magnetic field. In a mirror field this improves the axial confinement of the electrons. Following the heating, however, the electrons suffer collisions that slowly increase their parallel temperature at the expense of a decrease of their transverse temperature. They are then able to explore more deeply into the mirror regions. It should be noted that, as previously reported, the known spatial distribution of the electric field of the instability radiation is at a maximum and purely transverse to the static magnetic field at the midplane of the plasma.[4] At the maximum of the electric field the local electron-cyclotron frequency also equals the frequency of the instability radiation. Thus, this radiation should be quite effective in heating the electrons.

3. New Estimate of the Plasma Volume

Based on the assumption that the visible light provides a good measure of the spatial distribution of the plasma, a new estimate of the plasma volume has been made. From Fig. XI-7, the axial width of the light intensity at half maximum is 9.4 cm. At the midplane, Fig. XI-3 predicts that the radial extent of the intensity at half-maximum is 6.1 cm. Under the assumption that the plasma follows the static magnetic field lines, the result is an average radial extent of 5 cm over the length of the plasma. Thus, the new volume is estimated to be approximately 740 cc. It should be noted that this value is a factor of 12 smaller than that used by Fessenden.[5] Thus, the density values based on his estimate (which we had reported earlier) are a factor of 12 too low.

We are continuing both experimental and theoretical study of the plasma.

C. E. Speck

References

1. H. R. Griem, Plasma Spectroscopy (McGraw-Hill Book Company, New York, 1964), p. 176.
2. M. P. Freeman and S. Katz, "Determination of the Radial Distribution of Brightness in a Cylindrical Luminous Medium with Self-Absorption," J. Opt. Soc. Am. 50, 826 (1960).
3. H. Ikegami, I. Hiroyuki, M. Hosokawa, S. Tanaka, and K. Takayama, "Shell Structure of a Hot-Electron Plasma," Phys. Rev. Letters 19, 778-781 (October 1967).
4. C. Speck and A. Bers, "Experimental Study of Enhanced Cyclotron Radiation from an Electron-Cyclotron Resonance Discharge," Quarterly Progress Report No. 90, Research Laboratory of Electronics, M. I. T., July 15, 1968, pp. 134-135.
5. T. J. Fessenden, "Pulsed Electron-Cyclotron Resonance Discharge Experiment," Technical Report 442, Research Laboratory of Electronics, M. I. T., March 15, 1966, p. 31.

B. PLASMA INSTABILITIES IN A RESONANT CAVITY

Our recent experimental observations of a low-density plasma microinstability have shown that the microwave emission associated with the instability has a frequency that is almost identical to the resonant frequency of a high-Q mode of the cavity containing the plasma.[1] In this report we develop a theoretical model for understanding such microinstabilities. We consider the excitation of the cavity modes by the plasma currents, which in turn are related to the fields in the cavity in a self-consistent manner. We thus arrive at an equation for the characteristic complex frequencies of the cavity in the presence of the plasma.

It is well known that the electromagnetic fields in a cavity may be expressed in terms of a complete set of solenoidal and divergence modes.[2] Thus the electric field may be written

$$\bar{E}(\omega, \bar{r}) = \sum_{\kappa} V_{\kappa}(\omega)\, \bar{e}_{\kappa}(\bar{r}) \tag{1}$$

where $V_{\kappa}(\omega)$ are the amplitudes of the various modes (κ) and are determined by the sources, and $\bar{e}_{\kappa}(\bar{r})$ are the orthonormal vector-field distributions of the modes. The excitation of the modes by a current density distribution $\bar{J}(\omega, \bar{r})$ flowing inside the cavity volume (τ) is given by

$$V_{\nu} = \frac{j\omega/\epsilon\tau}{\omega^2 - \omega_{\nu}^2} \int_{cav} \bar{e}_{\nu}^{*}(\bar{r}) \cdot \bar{J}(\omega, \bar{r})\, d^3r \tag{2}$$

for solenoidal modes (ν), and by

$$V_{a} = \frac{j}{\omega\epsilon\tau} \int_{cav} \bar{e}_{a}^{*}(\bar{r}) \cdot \bar{J}(\omega, \bar{r})\, d^3r \tag{3}$$

for divergence modes (a), where the integral is over the cavity volume (cav)τ.

In a plasma the linearized current density is in general related to the electric field by a tensor conductivity operator,

$$\bar{J}(\omega, \bar{r}) = \bar{\bar{\sigma}}_{op}(\omega, \bar{r}) \cdot \bar{E}(\omega, \bar{r}), \tag{4}$$

which is in general an integral operator, to be discussed below. The electric field in Eq. 4 may be expressed in terms of the complete set of modes as in Eq. 1, and the excitation of the modes (Eqs. 2 and 3) is then given by

$$V_{\zeta} = C_{\zeta} \sum_{\kappa} V_{\kappa} \int_{cav} \bar{e}_{\zeta}^{*}(\bar{r}) \cdot \bar{\bar{\sigma}}_{op}(\omega, \bar{r}) \cdot \bar{e}_{\kappa}(\bar{r})\, d^3r, \tag{5}$$

where C_ζ is defined by Eqs. 2 and 3. Equation 5 is a homogeneous set of equations for the amplitudes of the modes

$$\sum_{\kappa'} V_{\kappa'} \left[\delta_{\kappa\kappa'} - C_\kappa \int_{cav} \bar{e}^*_\kappa(\bar{r}) \cdot \bar{\bar{\sigma}}_{op}(\omega, \bar{r}) \cdot \bar{e}_{\kappa'}(\bar{r})\, d^3r \right] = 0 \tag{6}$$

which has nontrivial solutions for

$$\det \left[\delta_{\kappa\kappa'} - C_\kappa \int_{cav} \bar{e}^*_\kappa(\bar{r}) \cdot \bar{\bar{\sigma}}_{op}(\omega, \bar{r}) \cdot \bar{e}_{\kappa'}(\bar{r})\, d^3r \right] = 0. \tag{7}$$

Equation 7 is the characteristic equation for the complex frequencies of the cavity-plasma system from which its stability may be determined.

For obtaining specific results Eq. 7 must be suitably approximated. To begin with, Eq. 7 is an infinite determinant involving the coupling of all of the modes. In the case of a low-density plasma which predominantly excites a high-Q cavity mode (nondegenerate), we may retain only the leading term in the expansion of Eq. 7 and find approximately

$$1 - C_\nu \int_{cav} \bar{e}^*_\nu(\bar{r}) \cdot \bar{\bar{\sigma}}_{op}(\omega, \bar{r}) \cdot \bar{e}_\nu(\bar{r})\, d^3r = 0, \tag{8}$$

where ν is the particular high-Q cavity mode with resonant frequency ω_ν, and the finite Q of the mode may be included in C_ν by replacing $\left(\omega^2 - \omega_\nu^2\right)$ by $\left(\omega^2 - j\omega\omega_\nu/Q_\nu - \omega_\nu^2\right)$. Equation 8 may be solved for the complex frequency $\omega = \omega_r + j\omega_i$ by perturbation techniques. Assuming $|\omega_i| \ll \omega_r$ and expanding the operator integral to first order, we find

$$\omega_r \cong \omega_\nu \tag{9}$$

$$\omega_i \cong \frac{\dfrac{\omega_\nu}{2Q_\nu} + \dfrac{1}{2\epsilon\tau} \displaystyle\int_{cav} \bar{e}^*_\nu \cdot \bar{\bar{\sigma}}^h_{op} \cdot \bar{e}_\nu\, d^3r}{1 + \dfrac{1}{2\epsilon\tau} \displaystyle\int_{cav} \bar{e}^*_\nu \cdot \frac{\partial\left(-j\bar{\bar{\sigma}}^a_{op}\right)}{\partial\omega} \cdot \bar{e}_\nu\, d^3r}, \tag{10}$$

where $\bar{\bar{\sigma}}^h_{op}$ and $\bar{\bar{\sigma}}^a_{op}$ are, respectively, the Hermitian and anti-Hermitian parts of $\bar{\bar{\sigma}}_{op}(\omega, \bar{r})$ evaluated at $\omega = \omega_\nu$. The integrals in the numerator and denominator of Eq. 10 are recognized as proportional to the time averaged power dissipated and energy stored associated with the plasma in the cavity mode fields,[3] respectively. In fact, Eq. 10 is identical to the result one would obtain directly from a generalized cavity mode

perturbation theory,[4]

$$\omega_i \approx \frac{P_\nu + P_{M\nu}}{2(W_\nu + W_{M\nu})}, \tag{11}$$

where P_ν and W_ν are the time-averaged power dissipated and energy stored in the cavity in the absence of plasma, and $P_{M\nu}$ and $W_{M\nu}$ are the time-averaged power dissipated and energy stored associated with the plasma medium; the subscript ν shows that these quantities are evaluated by using the unperturbed cavity mode fields. P_ν is associated with power dissipated in the cavity volume, walls, and passive terminations and is positive definite. Likewise, $W_\nu = \epsilon\tau|V_\nu|^2/2$ is a positive definite quantity. Hence instabilities can arise under either one of the following conditions:

(a) $W_{M\nu} + W_\nu > 0$ and $P_{M\nu} + P_\nu < 0$;

(b) $W_{M\nu} + W_\nu < 0$ and $P_{M\nu} + P_\nu > 0$.

Conditions (a) correspond to instabilities driven by "negative-dissipation" modes in the plasma, while conditions (b) correspond to instabilities due to "negative-energy" modes in the plasma. Conditions (b) are of particular interest to us, since our previous studies of collisionfree plasmas with anisotropic velocity distribution functions have uncovered numerous negative-energy waves,[5] and these in turn may fit some cavity mode fields, as in the case of our experiments.[1] In general, the frequency dependence of $\overline{\overline{\sigma}}_{op}$ contains resonances at Doppler-shifted cyclotron harmonic frequencies ($\omega \sim n\omega_c \pm \bar{k}\cdot\bar{v}$), and the characteristic equation may have to be evaluated to higher order in ω_i than in Eq. 10. This will be particularly true for relativistic instabilities[5] which resonate as $(\omega - n\omega_c \pm \bar{k}\cdot\bar{v})^2$.

Further specific results can be obtained by examining the linearized operator relation for the plasma current density, Eq. 4, in more detail. For an inhomogeneous and bounded plasma this may be written

$$\bar{J}(\omega, \bar{r}) = \int d^3r' \, \overline{\overline{\sigma}}(\omega, \bar{r}, \bar{r}') \cdot \bar{E}(\omega, \bar{r}'), \tag{12}$$

where specific boundary conditions may be included in both the limits of integration and the form of the tensor $\overline{\overline{\sigma}}$. For wavelengths that are short compared with both the scale of the inhomogeneity and the cavity dimensions, we can approximate Eq. 12 by

$$\begin{aligned}\bar{J}(\omega, \bar{r}) &\cong \int d^3r' \, \overline{\overline{\sigma}}(\omega, \bar{r}-\bar{r}') \cdot \bar{E}(\omega, \bar{r}') \\ &= \int \frac{d^3k}{(2\pi)^3} e^{-j\bar{k}\cdot\bar{r}} \, \overline{\overline{\sigma}}(\omega, \bar{k}) \cdot \bar{E}(\omega, \bar{k})\end{aligned} \tag{13}$$

(or in a WKB equivalent version). With these approximations the integral in the characteristic equation for the complex frequencies, Eq. 7, becomes

$$\int_{cav} \bar{e}^*_\kappa(\bar{r}) \cdot \bar{\bar{\sigma}}_{op}(\omega, \bar{r}) \cdot \bar{e}_{\kappa'}(\bar{r})\, d^3r$$

$$\simeq \int \frac{d^3k}{(2\pi)^3}\, \bar{e}^*_\kappa(\bar{k}) \cdot \bar{\bar{\sigma}}(\omega, \bar{k}) \cdot \bar{e}_{\kappa'}(\bar{k}), \tag{14}$$

where $\bar{e}_\kappa(\bar{k})$ is the Fourier transform of $\bar{e}_\kappa(\bar{r})$. If we express the cavity mode fields $\bar{e}_\kappa(\bar{r})$ in terms of a superposition of plane waves, the integration in Eq. 14 can be readily carried out. Equation 14 is then expressed as a sum of specific elements of the conductivity tensor which are picked out by the field distribution of the cavity mode and evaluated at the wave numbers pertinent to the mode. Thus our extensive studies of $\bar{\bar{\sigma}}(\omega, \bar{k})$ for plasmas with anisotropic velocity distribution functions[5] can be used to determine the stability of a resonant cavity system containing such a plasma. The detailed effects of inhomogeneities in plasma density and applied magnetic field, and of boundaries, will require further studies for determining suitable approximations in the evaluation of the conductivity operator and the integral in Eq. 7.

A. Bers

References

1. C. E. Speck and A. Bers, Quarterly Progress Report No. 90, Research Laboratory of Electronics, M.I.T., July 15, 1968, p. 135.
2. J. C. Slater, Microwave Electronics (McGraw-Hill Book Company, New York, 1950).
3. W. P. Allis, S. J. Buchsbaum, and A. Bers, Waves in Anisotropic Plasmas (The M.I.T. Press, Cambridge, Mass., 1963), see Sec. 8.5.
4. F. Gardiol and A. Bers, Quarterly Progress Report No. 77, Research Laboratory of Electronics, M.I.T., April 15, 1965, p. 153.
5. A. Bers and C. E. Speck, Quarterly Progress Report No. 81, Research Laboratory of Electronics, M.I.T., April 15, 1966, p. 133; Quarterly Progress Report No. 82, July 15, 1966, p. 189; E. Robertson and A. Bers, Quarterly Progress Report No. 79, October 15, 1965, p. 107.